Hindawi Publishing Corporation
Advances in Materials Science and Engineering
Volume 2014, Article ID 421729, 9 pages
http://dx.doi.org/10.1155/2014/421729

Research Article

Mesostructural Design and Manufacturing of Open-Pore Metal Foams by Investment Casting

Alexander Martin Matz,[1,2] Bettina Stefanie Mocker,[2] Daniel Wyn Müller,[2] Norbert Jost,[2] and Gunther Eggeler[1]

[1] *Institute for Materials, Ruhr-University Bochum, Universitätsstraße 150, 44780 Bochum, Germany*
[2] *Institute for Materials and Material Technologies, Pforzheim University of Applied Sciences, Tiefenbronner Straße 65, 75175 Pforzheim, Germany*

Correspondence should be addressed to Alexander Martin Matz; alexander.matz@ruhr-uni-bochum.de

Received 11 October 2013; Accepted 12 March 2014; Published 15 April 2014

Academic Editor: Thomas Hipke

The present paper describes the manufacturing process of open-pore metal foams by investment casting and the mesostructural/morphological evolution resulting from a new technique of modifying the precursor. By this technique, the precursor is coated with a polymer layer whereby a thickening of the struts occurs. Relative densities in the range of $1.85 \leq \rho_{rel} \leq 25\%$ of open-pore metal foams can be achieved with high accuracy. The samples investigated have pore densities of $\rho_P = 7$ ppi, 10 ppi, and 13 ppi. The relevant processing parameters needed for a homogenous formation of the polymer layer are determined for two different coating materials and the resulting open-pore foam's mesostructure is characterized qualitatively and quantitatively. The alloy used for investment casting open-pore metal foamsis AlZn11. The microstructural evolution of these foams is evaluated as a function of the mesostructure. Differences in the microstructure are observed for foams with low and high relative densities and discussed in terms of cooling subsequent to investment casting.

1. Introduction

Open-pore metal foams possess attractive properties due to their highly porous and light weight structure in combination with their base material. Hence, this group of materials is of great interest for different fields of application, such as in the sectors of heat engineering [1, 2], biomedical engineering [3, 4], electrical energy storage [5, 6], or lightweight design [7, 8].

Common processing techniques for manufacturing open-pore metal foams are based on sintering or casting [9, 10]. The method used in this investigation is a modified investment casting process which offers great advantages due to a targeted adaptation/tailoring of the relative density ρ_{rel}, structure of the cells, geometry, and alloy composition for any specific application. The open-pore metal foam also acts as an exact copy of the precursor—whereby also highly complex component geometries are possible—, and regular structures and pore-size distributions can be achieved [11–13]. Typically, a reticulated polymer foam [14] is used as a precursor. In many investigations (cf. [15–17]) these polymer foams are used for the metal foam production in as-received conditions leading to a relative density of $\rho_{rel} = 2 \pm 0.2\%$ for samples in a range of pore densities of $10\,\text{ppi} \leq \rho_P \leq 40\,\text{ppi}$. However, for some applications such a low metallic portion is not adequate and hence the relative density needs to be enhanced. One common method of doing this is by thickening the struts of the polymer foam by dunking it into liquid wax [16, 18–20]. However, this method requires a high level of experience to achieve a homogenous structure in a repetitive accuracy and to avoid blocking of the pores [18, 19]. Furthermore, thickening the struts can just be conducted within narrow confines.

For these reasons an alternative method for a mesostructural design of open-pore metal foams is developed. Using this method any required relative density ρ_{rel} can be achieved through a homogenous thickening of the struts. The

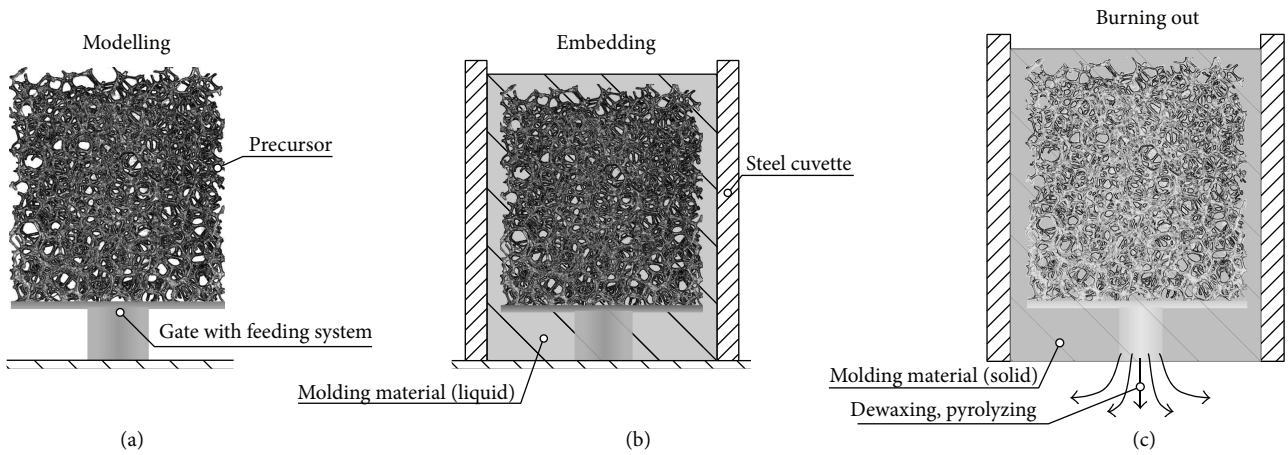

Figure 1: Schematic diagram of mold preparation process: (a) modelling in terms of mounting precursor on gate with feeding system, (b) embedding in terms of infiltrating the pattern placed in a steel cuvette by molding material, and (c) burning out in terms of dewaxing the gating system, pyrolyzing the precursor, and hardening the mold.

thickening is a thermal-additive process where the struts of the samples are firstly coated with an adhesive layer, followed secondly by powdering them with polymer granules and thirdly treating the samples above the melting temperature ϑ_M of the polymer granules. In the present study the basics of the modified investment casting process for open-pore metal foams are described briefly. Furthermore, the influence of treatment time t_{th}, treatment temperature ϑ_{th}, diameter of polymer granules d_p, and quantity of treatment runs n_{th} on the open-pore metal foam's mesostructure and its relative density ρ_{rel} is investigated. The microstructural evolution resulting in the investment casted open-pore metal foams is identified.

2. Experimental

2.1. Strut Thickening. The precursors for the modified investment casting process used in this investigation are commercial reticulated open-pore polymer foams (brand name "Regicell") with different pore densities of $\rho_P = 7$ ppi, 10 ppi, and 13 ppi, obtained from Foampartner Reisgies Schaumstoffe GmbH in Leverkusen, GER. These as-received samples have a relative density of $\rho_{\text{rel}} = 1.95 \pm 0.05\%$ representing the reference condition for this study. The thickening of the open-pore polymer foam's struts as a three-step process is achieved via the following:

(1) spray coating with a synthetic elastomer based aerosol glue with the brand name "Scotch-Weld Spray 77" from 3 M Deutschland GmbH in Neuss, GER as an adhesive layer in an apparatus with a rotating sample holder at standard conditions, resulting in a homogenous distribution of the adhesive on the polymer foam's surface,

(2) powdering with polymer granules in diameters of $d_p \approx 290\,\mu$m (PG1) of the type Abcite X1060 from DuPont Polymer Powders Switzerland Sàrl in Bulle, CH and $d_p \approx 32\,\mu$m (PG2) of the type FA-7035-SG412 from Ganzlin Beschichtungspulver GmbH in Ganzlin, GER in the abovementioned apparatus at standard conditions, resulting in a homogenous distribution of the polymer granule on the polymer foam's spray coated surface, and

(3) thermal treatment of the coated samples in a batch furnace at $\vartheta_{\text{th}} = 160^{\circ}$C for $t_{\text{th}} = 14$ min (PG1) or $t_{\text{th}} = 12$ min (PG2), respectively, followed by cooling at standard conditions.

2.2. Mold Preparation. The precursor in its dimensions of $50 \cdot 50 \cdot 20\,\text{mm}^3$ is mounted on a gate with a feeding system made of wax which represents the pattern in its final state (Figure 1). Thereupon this pattern is placed in a steel cuvette. The molding material is a sulfate-bonded investment, supplied by SRS Ltd. in Riddings, GB, which is mixed with water and stirred to form a ceramic slurry which gets evacuated until reaching a residual pressure of $p \approx 25$ mbar to minimize trapped air. After drying for $t = 1$ h at standard conditions, the mold is heated in an incineration furnace in a multistep cycle, shown in Figure 2. The first step at a temperature of $\vartheta = 110^{\circ}$C is conduced to counteract the hygroscopicity. In a second step at $\vartheta = 240^{\circ}$C the gating system is dewaxed and in a third step at $\vartheta = 360^{\circ}$C the polymeric precursor is pyrolyzed. The final drying and hardening of the mold is achieved at $\vartheta = 720^{\circ}$C in a last step followed by furnace cooling. Due to phase transitions and volume changes, these temperatures are kept for at least $t = 1.5$ h and a heating rate of max. $T/t = 6$ K/min is chosen to prevent crack formation.

2.3. Casting. The alloy used for all castings in this study is AlZn11. The starting materials are Al granules with a purity of ≥99,99% and Zn pieces with a purity of ≥99,995% from Chempur Feinchemikalien und Forschungsbedarf GmbH in Karlsruhe, GER. The metallurgical processing of the open-pore metal foam is carried out by centrifugal casting. Both,

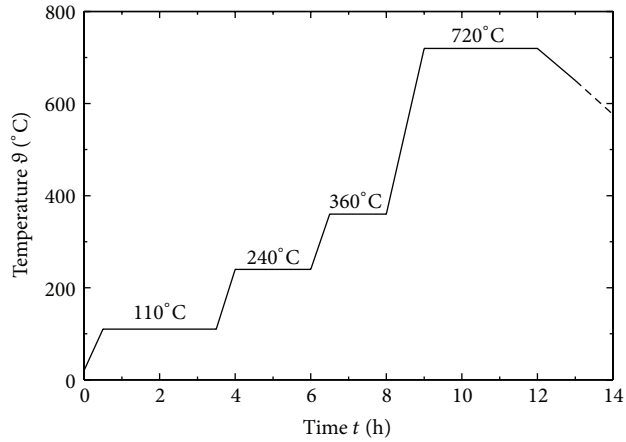

Figure 2: Process of dewaxing, pyrolyzing, and mold hardening.

Al and Zn in the mass ratio $m_{Al}/m_{Zn} = 89/11$, are placed in a preheated crucible and inductively melted under vacuum. At a temperature of $\vartheta = 750^{\circ}C$, the casting is induced and the mold, which was preheated at $\vartheta = 650^{\circ}C$ for $t = 5$ h, is infiltrated by the melt. After $t = 3$ min, the mold is removed from the casting machine whereupon it is quenched in water ($\vartheta = 20^{\circ}C$). In a last step the samples are cleaned by water jet and Tetranatriumethylendiamintetraacetate ($C_{10}H_{12}N_2Na_4O_8$).

2.4. Mesostructural Characterization. The mesostructure of open-pore foams includes the geometric parameters of the foam-like structure such as strut width s_{st} and cell diameter d_c and general foam parameters including pore density ρ_P and relative density ρ_{rel}. To determine the effects of strut thickening on the foam's mesostructure, the digital microscope "VHX-500FD" from Keyence NV/SA in Mechelen, BEL, is used. The conducted investigations are focused on the degree of wetting of the struts by the polymer layer and the interaction of successively added polymer granules, which is analyzed qualitatively. Furthermore, quantitative correlations of polymer granules diameterd_p, strut width s_{st}, and relative density ρ_{rel} are deduced. The relative density, which is defined as

$$\rho_{rel} = \frac{m_f}{m_s}, \tag{1}$$

the ratio of the foam's mass m_f and the mass of a solid body m_s with the same base material in identical outer dimensions, is governed by weighing the open-pore AlZn11 foam sample with a microbalance (type "AB104" from Mettler-Toledo GmbH in Gießen, GER).

2.5. Microstructural Characterization. To evaluate the influence of the relative density ρ_{rel} on the microstructural evolution of the open-pore AlZn11 foams, microscopical studies are carried out. Therefore, the metal foam samples are partitioned at a distance of $s = 25$ mm to the deadhead by a wet disc grinder. The single sample pieces are embedded in a cold polymerizing plastic (Scandiplex in addition to Varioplex from Scan-Dia Hans-P. Tempelmann GmbH & Co.KG in Hagen, GER) for further mechanical sample preparation. This is carried out by an automatic grinding/polishing machine (TegraPol-21 from Struers GmbH, GER) in two main steps, namely, wet grinding and diamond polishing as well as chemic-mechanical polishing, as described in [21] in detail. Subsequent to these preliminary steps, electrolytic etching according to Barker is applied (cf. [22]). The microscopical studies of the prepared samples are obtained by a light-optical microscope (DMI 500 M from Leica GmbH, GER) at amplifications of $V = 100 : 1$ in polarized light for evaluating the microstructural morphology.

3. Results and Discussion

In the following, the results of the experimental investigations are pointed out. The processing quality is examined to determine the optimum processing parameters for strut thickening and the mesostructural evolution is characterized by quantifying mesostructural parameters. Moreover, the microstructural evolution in consequence of the varied mesostructure is evaluated for the investment casted foam samples.

3.1. Processing Quality. The key factors for the mesostructural design of open-pore metal foams are the processing parameters of the thermal-additive method for thickening the struts. Particularly temperature ϑ_{th} and time t_{th} of thermal treatment affect the quality of the precursor considerably.

As basic conditions for identifying the optimum thermal treatment temperature ϑ_{th}, the chosen temperature needs to exceed the melting temperature $\vartheta_{th} > \vartheta_M$ of the polymer granules or coating material, respectively, and needs to be below the temperature where the skeletal structure of the polymer foam collapses, $\vartheta_{th} < \vartheta_c$. According to manufacturer's data and DSC measurements the relevant temperatures for both polymer granules ϑ_M and the polymer foam ϑ_c are determined. The melting temperature is $\vartheta_M \approx 93^{\circ}C$ for PG1 and $\vartheta_M \approx 95^{\circ}C$ for PG2. The foam proves to be inherently stable until reaching a temperature of $\vartheta_c \approx 255^{\circ}C$.

In a series of experiments, thermal treatment in a temperature range of $120^{\circ}C \leq \vartheta_{th} \leq 200^{\circ}C$ was conducted. The results show at $\vartheta_{th} \lesssim 155^{\circ}C$ that the desired effect of strut thickening can be achieved. However, the process needs up to half an hour to be finished. At $\vartheta_{th} \gtrsim 165^{\circ}C$, the process can be accelerated which is yet coupled with the negative side effect of mass stratification of the polymer layer due to gravitation and a nonhomogenous relative density within the foam, respectively. The best results are determined to be at $\vartheta_{th} = 160^{\circ}C$ for PG1 and PG2.

The required duration of the thermal treatment is investigated in another series of experiments. For this purpose several polymer foam samples are prepared using the first and second process step mentioned in Section 2.1 and thermal treatment at $\vartheta_{th} = 160^{\circ}C$ in a time range of $4\,\text{min} \leq t_{th} \leq 14\,\text{min}$ is applied, whereby all minute samples are taken and qualitatively analyzed by the digital microscope. The evolution of strut thickening is shown in Figure 3 which demonstrates the formation of a polymer layer

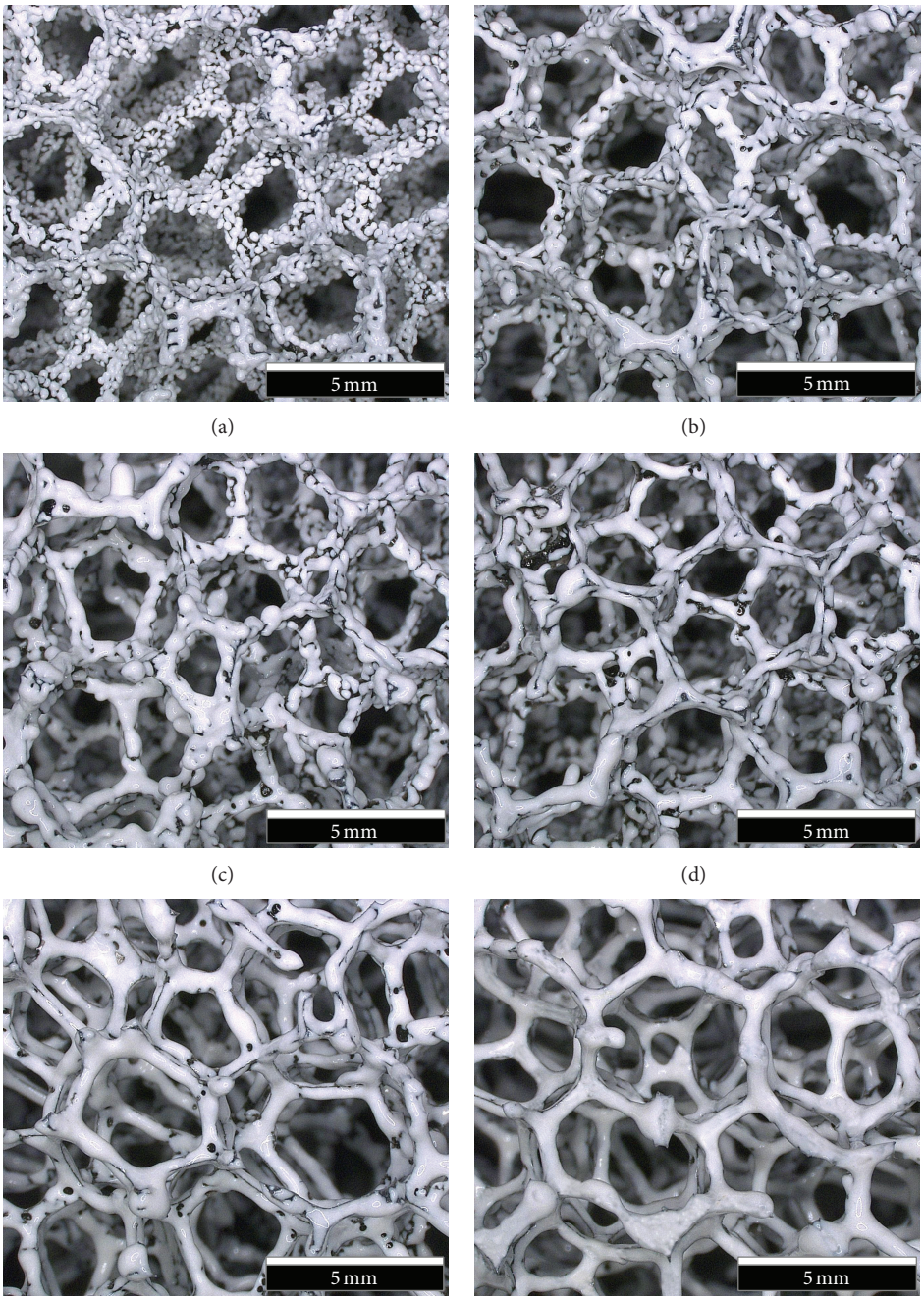

Figure 3: Evolution of strut thickening by PG1 at $\vartheta_{th} = 160^{\circ}C$ after thermal treatment of (a) $t_{th} = 4$ min, (b) $t_{th} = 6$ min, (c) $t_{th} = 8$ min, (d) $t_{th} = 10$ min, (e) $t_{th} = 12$ min, and (f) $t_{th} = 14$ min using the example of a polymer foam with a pore density of $\rho_P = 10$ ppi.

by agglomeration of the single powder granules as a function of time leading to the result of a homogenous layer after $t_{th} = 14$ min for PG1. Using PG2, a homogenous layer is formed after $t_{th} = 12$ min.

3.2. Mesostructural Evolution. To quantify the mesostructural evolution aroused by the thermal-additive process for strut thickening, all the polymer foam samples are characterized in consideration of the overall mesostructural key parameter: the relative density ρ_{rel}. It can be observed that ρ_{rel} is in a linear relationship as a function of the quantity of thermal treatment runs n_{th}, as shown in Figure 4. By comparing the pore densities ρ_P of the foam samples, it can be seen that the increase in relative density $\Delta\rho_{rel}$ with each treatment run n_{th} rises by a higher pore density ρ_P or a smaller cell diameter d_c, respectively. An increase of pore density by $\Delta\rho_P = 3$ ppi leads to an approx. 0.325% higher relative density per treatment $\Delta\rho_{rel}/n_{th}$.

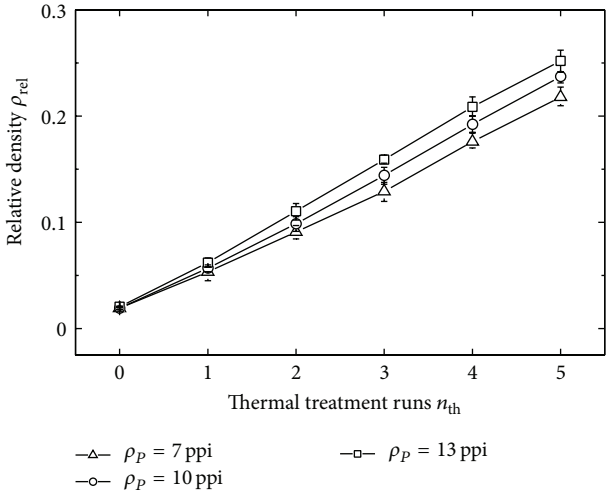

Figure 4: Relative density ρ_{rel} as a function of the quantity of thermal treatment runs n_{th} of strut thickened (by PG1) polymer foams with pore densities of ρ_P = 7 ppi, 10 ppi, and 13 ppi.

This can be explained by considering the specific surface area of the foam which is available for coating by the polymer powder. Using the example of a simple expression for the specific surface area

$$\xi_f = \frac{c_1}{d_c}, \tag{2}$$

(see [23, 24]) with c_1 as a constant and d_c as the cell diameter and the relation between the relative density and cell diameter

$$d_c = \frac{c_2}{\rho_P}, \tag{3}$$

with c_2 as another constant and inserting (2) in (3) leads to the relation

$$\xi_f \propto \rho_P, \tag{4}$$

between the specific surface area and pore density with the consequence of a higher relative density by increasing the pore density.

As another mesostructural parameter, the strut width s_{st} is characterized by measuring the distance between the outer edges of a single strut, as the example depicted by Inayat et al. [23]. In each sample batch with identical pore density ρ_P and identical quantity of thermal treatment runs n_{th}, at least 150 single struts are measured to achieve a representative mean value, since the mesostructural parameters, such as the strut width, are normally distributed [23]. For a sample batch with ρ_P = 10 ppi, which was treated by n_{th} = 2 runs with PG1 (resulting in a relative density of ρ_{rel} = 9.86%), the strut width distribution is shown in Figure 5. The mean value of the strut width is s_{st} = 0.834 mm and the standard deviation amounts to σ_{st} = 0.037 mm for this foam. The corresponding strut widths resulting for the other samples coated by PG1 are listed in Table 1 and the ones coated by PG2 are listed in Table 2.

The increase in strut width s_{st} shows, similarly to the relative density ρ_{rel}, that it is in a linear conjunction with the

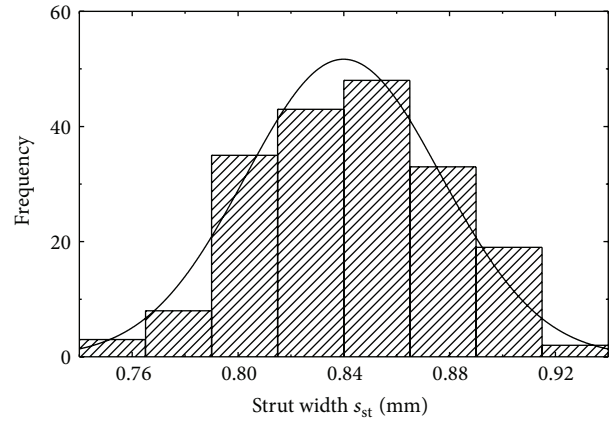

Figure 5: Strut width distribution of open-pore foams with a pore density of ρ_P = 10 ppi and a relative density of ρ_{rel} = 9.86%.

Table 1: Mesostructural parameters of strut thickened polymer foams by PG1.

Pore density ρ_P (ppi)	Quantity of thermal treatment runs n_{th}	Relative density ρ_{rel}	strut width s_{st} (mm)
7	0	0.01922	0.362
7	1	0.05335	0.595
7	2	0.09088	0.849
7	3	0.12906	1.190
7	4	0.17593	1.536
7	5	0.21794	1.820
10	0	0.01918	0.322
10	1	0.05694	0.541
10	2	0.09857	0.834
10	3	0.14421	1.141
10	4	0.19211	1.423
10	5	0.23721	1.797
13	0	0.02060	0.278
13	1	0.06205	0.531
13	2	0.11053	0.796
13	3	0.15899	1.011
13	4	0.20870	1.383
13	5	0.25196	1.706

quantity of thermal treatment runs n_{th} and can be expressed by

$$s_{st,x} \approx d_p \cdot n_{th} + s_{st,0} \tag{5}$$

in which the strut width resulting for any thermal treatment run $s_{st,x}$ increases by the product of the polymer granule's particle diameter d_p and the quantity of thermal treatment runs n_{th}. However, this expression is, in this investigation, only valid for the polymer granule PG1. For the other polymer granule, PG2, the function

$$s_{st,x} \approx \begin{cases} s_{st,0} & n_{th} \leq 2 \\ d_p \cdot n_{th} + s_{st,0} & n_{th} > 2 \end{cases} \tag{6}$$

Table 2: Mesostructural parameters of strut thickened polymer foams by PG2.

Pore density ρ_P (ppi)	Quantity of thermal treatment runs n_{th}	Relative density ρ_{rel}	strut width s_{st} (mm)
10	0	0.01918	0.322
10	1	0.02296	0.320
10	2	0.02803	0.325
10	3	0.03210	0.360
10	4	0.03592	0.391
10	5	0.04162	0.420
10	6	0.04510	0.438
10	7	0.04860	0.486
10	8	0.05361	0.507
10	9	0.05921	0.554
10	10	0.06412	0.587

results. This can be justified by the small particle diameter d_p of PG2 (compared to PG1) which forms just a thin polymer layer on the foam's surface in conjunction with the fact that the polymer foam in reference conditions or untreated conditions ($n_{th} = 0$), respectively, exhibits a strut cross section which can be described by a concaved equilateral triangle (Plateau border). Treating the polymer foam by $n_{th} = 1$, its strut cross sections result in an equilateral triangle (Figure 6(a)) and by $n_{th} = 2$ the strut cross sections become shaped as a convex equilateral triangle (Figure 6(b)). In all three conditions, $n_{th} = 0$, 1, and 2, the outer tips of the plateau border remain as the outer edges by applying the above named method for measuring, resulting in an identical strut width s_{st}. In comparison, a strut of a polymer foam treated by $n_{th} = 3$ is shown in Figure 6(c) at which the strut cross section emerges in a circular-like shape.

Furthermore, it can be deduced from Table 1 that a lower pore density ρ_P leads to a higher strut width s_{st} for each treatment run. This fact results due to the already higher strut width s_{st} of low-pore density foams in untreated or as-received conditions as the consequence of a lower amount of struts in total by an approx. identical relative density ρ_{rel}.

3.3. Microstructural Evolution. The evaluation of the microstructural evolution as a result of the varied mesostructural parameters is investigated for the open-pore AlZn11 foams with a pore density of $\rho_P = 10$ ppi. The sample illustrated in Figure 7(a) represents the reference conditions and is hence not strut thickened ($n_{th} = 0$). The ones shown in Figures 7(b) and 7(c) are strut thickened by a quantity of thermal treatment runs $n_{th} = 3$ and $n_{th} = 5$ with PG1. The increase in strut width with each treatment run $\Delta s_{st}/n_{th}$ can be seen clearly through these macroscopic photographs.

Sample preparation and metallographic analysis are applied as mentioned in Section 2.5 whereby the investigated sections of the foam represent a strut orientated parallel to the sample plane. The micrograph illustrated in Figure 8(a) shows a strut in untreated conditions ($n_{th} = 0$) with two comparatively large grains. In contrast, in the investigated sections of the samples strut thickened with PG1 by $n_{th} = 5$ (Figure 8(c)), a dominant dendritic microstructure with small grains is visible. The samples treated by $n_{th} = 3$ (Figure 8(b)) partly exhibit a distinctive dendritic microstructure and there are partial zones at which no casting structure is evident.

These differences in microstructure can be explained by the fact that after solidification in the mold, the cooling rate is higher in foam samples with a higher relative density since a higher volume fraction of AlZn11 is existent and more heat can be dissipated due to the high thermal conductivity λ of an Al alloy. In contrast, the thermal conductivity of the plaster is much smaller but its heat capacity c_p is much higher which leads to a lower heat dissipation in foams with small relative densities ρ_{rel}.

4. Summary and Conclusion

In the present study, a new method of thickening the struts is proposed to achieve defined relative densities of investment-cast open-pore metal foams in the range of $1.85\% \leq \rho_{rel} \leq 25\%$. This method is a three-step process, where the open-pore polymer foams need to get spray coated by an adhesive layer, afterwards powdered with polymer granules, and thermally treated to achieve a precursor in its required relative density with homogenous struts. Subsequently, the common procedure of investment casting has to be applied.

For evaluating the processing quality of the strut thickening process, two polymer powders with different particle diameters $d_p \approx 290\,\mu$m (PG1) and $d_p \approx 32\,\mu$m (PG2) are investigated. By varying temperature ϑ_{th} and time t_{th} of thermal treatment, the optimum parameters for a homogenous mesostructure of the foam and for a uniform formation of the polymer layer are identified. The processing temperature is determined to be at $\vartheta_{th} = 160^{\circ}$C for both powder types. The formation of the polymer layer occurring by agglomeration of the powder granules is achieved after $t_{th} = 14$ min for PG1 and $t_{th} = 12$ min for PG2.

With respect to the mesostructural parameters resulting from this method, the relative density ρ_{rel} and strut widths s_{st} as a function of the quantity of thermal treatment runs n_{th} are determined for open-pore foams with pore densities of $\rho_P = 7$ ppi, 10 ppi, and 13 ppi. A linear relationship between ρ_{rel} and n_{th} is observed whereby the increase of ρ_{rel} with each treatment run is more dominant as the pore density ρ_P is higher which is a consequence of the foam's specific surface area ξ_f. Furthermore, the strut widths s_{st} also show a linear dependency on the quantity of thermal treatment runs n_{th} in compliance with the requirement of a circular-like shaped strut cross section which can be ascribed by the product of the polymer powder's particle diameters ρ_P and quantity of thermal treatment runs n_{th} in addition to the strut width of the foam in untreated conditions $s_{st,0}$.

The microstructural evaluation indicates differences in the microstructure of the open-pore AlZn11 foams as a function of the mesostructural parameters. A dominant dendritic structure in foams with high relative densities is

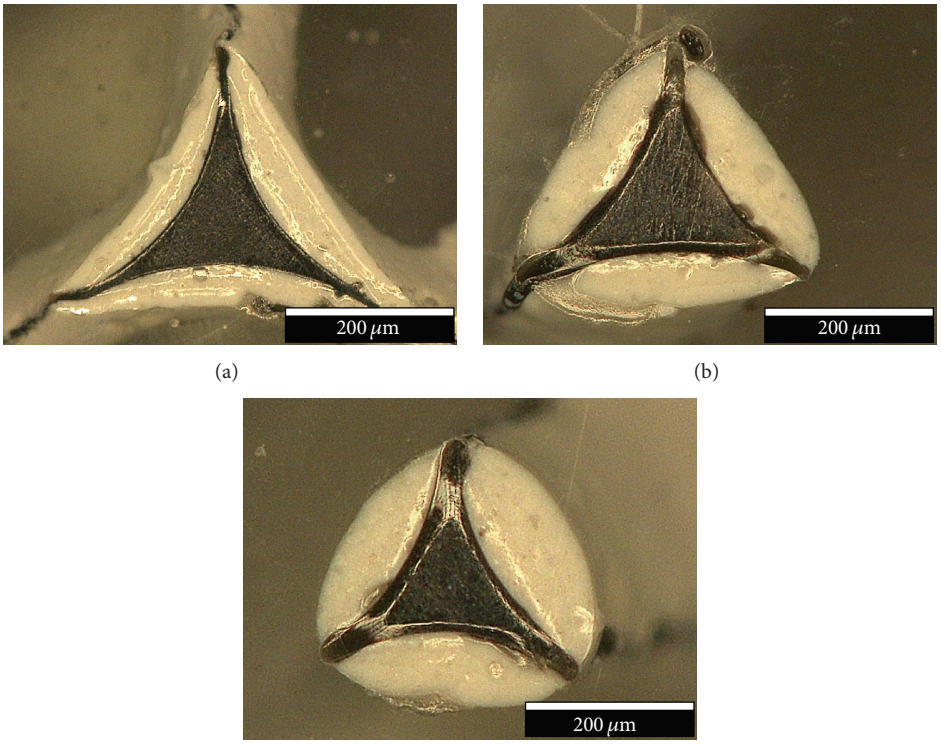

(a) (b)

(c)

FIGURE 6: Cross section of a single strut of a PG2-treated polymer foam with a pore density of $\rho_P = 10$ ppi by a quantity of thermal treatment runs of (a) $n_{th} = 1$, (b) $n_{th} = 2$, and (c) $n_{th} = 3$.

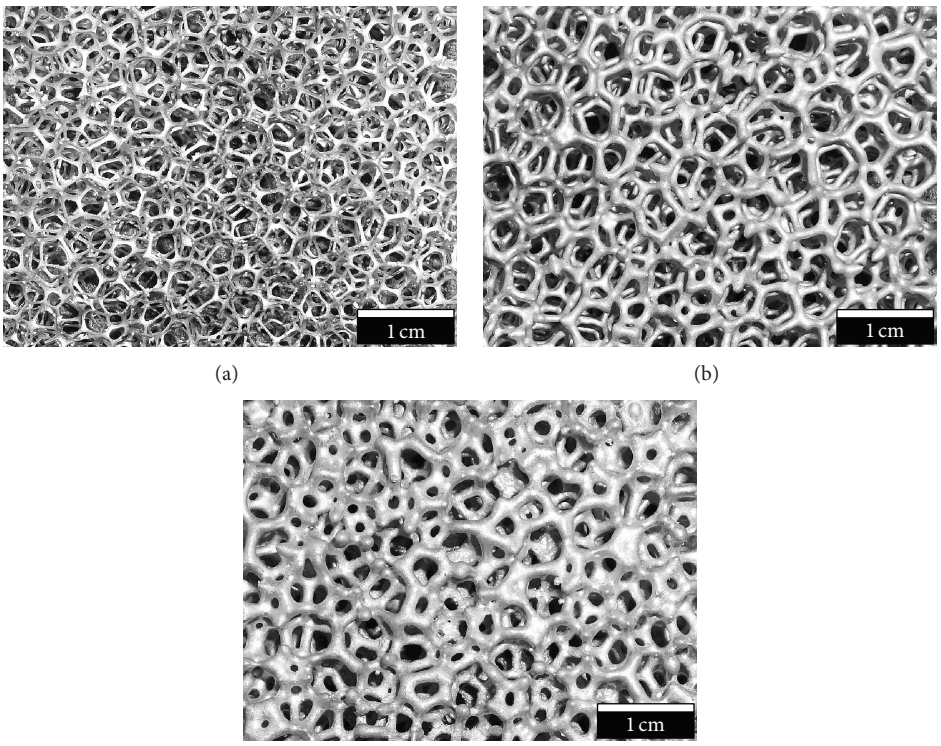

(a) (b)

(c)

FIGURE 7: Open-pore AlZn11 foams with a pore density of $\rho_P = 10$ ppi (a) in untreated conditions ($n_{th} = 0$), (b) strut thickened with PG1 by $n_{th} = 3$, and (c) strut thickened with PG1 by $n_{th} = 5$.

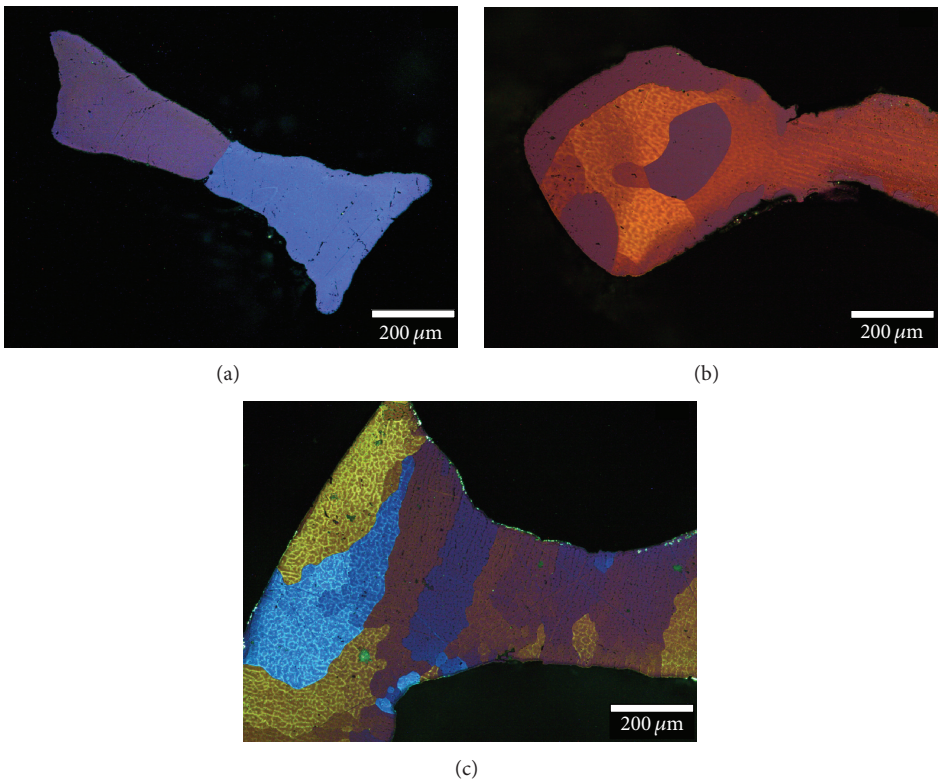

(a) (b)

(c)

FIGURE 8: Microstructure of open-pore AlZn11 foams (a) in untreated conditions ($n_{th} = 0$), (b) with PG1 strut thickened by $n_{th} = 3$, and (c) with PG1 strut thickened by $n_{th} = 5$.

observed whereas no indications for that are evident in foams with low relative densities. The reason might be a higher cooling rate resulting from the higher metal portion with its high thermal conductivity in foams with high relative densities.

Conflict of Interests

The authors declare that there is no conflict of interests regarding the publication of this paper.

Acknowledgments

The authors gratefully acknowledge the European Union/European Fund for Regional Development and the federal state Baden-Württemberg for financial support. Moreover, they wish to thank Foampartner Reisgies Kunststoffe GmbH, especially H.-J. Stolz, DuPont Polymer Powders Switzerland Sàrl, and Ganzlin Beschichtungspulver GmbH for material support. The authors would also like to express their gratitude to E. Drotleff, R. Burkart, and J. Aktas for assistance concerning experimental tasks.

References

[1] X.-H. Han, Q. Wang, Y.-G. Park, C. T'Joen, A. Sommers, and A. Jacobi, "A review of metal foam and metal matrix composites for heat exchangers and heat sinks," *Heat Transfer Engineering*, vol. 33, no. 12, pp. 1–20, 2012.

[2] C. Y. Zhao, "Review on thermal transport in high porosity cellular metal foams with open cells," *International Journal of Heat and Mass Transfer*, vol. 55, no. 13-14, pp. 3618–3632, 2012.

[3] Y. Er and E. Unsaldi, "The production of nickel-chromium-molybdenum alloy with open pore structure as an implant and the investigation of its biocompatibility in vivo," *Advances in Materials Science and Engineering*, vol. 2013, Article ID 568479, 7 pages, 2013.

[4] D. W. Müller, A. M. Matz, and N. Jost, "Casting open porous Ti foam suitable for medical applications," *Bioinspired, Biomimetic and Nanobiomaterials*, vol. 2, no. 2, pp. 76–83, 2013.

[5] P. S. Liu, T. F. Li, and C. Fu, "Relationship between electrical resistivity and porosity for porous metals," *Materials Science and Engineering A*, vol. 268, no. 1-2, pp. 208–215, 1999.

[6] Q.-X. Low, W. Huang, X.-Z. Fu et al., "Copper coated nickel foam as current collector for H_2S-containing syngas solid oxide fuel cells," *Applied Surface Science*, vol. 258, no. 3, pp. 1014–1020, 2011.

[7] M. F. Ashby, "The mechanical properties of cellular solids," *Metallurgical Transactions A*, vol. 14, no. 9, pp. 1755–1769, 1983.

[8] H. Kanahashi, T. Mukai, Y. Yamada et al., "Experimental study for the improvement of crashworthiness in AZ91 magnesium foam controlling its microstructure," *Materials Science and Engineering A*, vol. 308, no. 1-2, pp. 283–287, 2001.

[9] G. J. Davies and S. Zhen, "Metallic foams: their production, properties and applications," *Journal of Materials Science*, vol. 18, no. 7, pp. 1899–1911, 1983.

[10] H. N. G. Wadley, "Cellular metals manufacturing," *Advanced Engineering Materials*, vol. 4, no. 10, pp. 726–733, 2002.

[11] S. F. Fischer, M. Thielen, R. R. Loprang et al., "Pummelos as concept generators for biomimetically inspired low weight structures with excellent damping properties," *Advanced Engineering Materials*, vol. 12, no. 12, pp. B658–B663, 2010.

[12] A. Jung, *Offenporige, nanobeschichtete hybrid-metallschäume: herstellung und mechanische eigenschaften [Ph.D. dissertation]*, Saarland University, Saarbrücken, Germany, 2011, (German).

[13] U. Krupp, A. Ohmdorf, T. Guillén et al., "Isothermal and thermomechanical fatigue behavior of open-cell metal sponges," *Advanced Engineering Materials*, vol. 8, no. 9, pp. 821–827, 2006.

[14] R. A. Volz, "Reticulated polyurethane foams and process for their production," US3171820, 1965.

[15] S. F. Fischer, P. Schüler, C. Fleck, and A. Bühring-Polaczek, "Influence of the casting and mould temperatures on the (micro)structure and compression behaviour of investment-cast open-pore aluminium foams," *Acta Materialia*, vol. 61, no. 14, pp. 5152–5161, 2013.

[16] L. C. Wang and F. Wang, "Preparation of the open pore aluminum foams using investment casting process," *Acta Metallurgica Sinica (English Letters)*, vol. 14, no. 1, pp. 27–32, 2001.

[17] Y. Yamada, K. Shimojima, Y. Sakaguchi et al., "Processing of an open-cellular AZ91 magnesium alloy with a low density of 0.05 g/cm^3," *Journal of Materials Science Letters*, vol. 18, no. 18, pp. 1477–1480, 1999.

[18] M. Grohn, *Feingegossene metallschwämme als preform zur schmelzflüssigen infiltration [Ph.D. dissertation]*, Shaker, Aachen, Germany, 2005, (German).

[19] C. A. Hintz, *Präzisionsgegossene metallische schwammstrukturen [Ph.D. dissertation]*, Shaker, Aachen, Germany, 2003, (German).

[20] L. Wang, H. Li, F. Wang, and J. Ren, "Preparation of open-cell metal foams by investment cast," *China Foundry*, vol. 2, no. 1, pp. 56–59, 2005.

[21] B. S. Mocker, U. Christian, A. M. Matz, N. Jost, and C. Siegle, "Mikrostrukturelle charakterisierung im feingussverfahren hergestellter offenporiger metallschäume aus aluminium-silizium-legierungen," *Fortschritte in der Metallographie*, vol. 45, pp. 279–284, 2013 (German).

[22] G. Petzow, *Metallographic Etching: Techniques for Metallography, Ceramography, Plastography*, ASM International, Materials Park, Ohio, USA, 2nd edition, 2001.

[23] A. Inayat, H. Freund, T. Zeiser, and W. Schwieger, "Determining the specific surface area of ceramic foams: the tetrakaidecahedra model revisited," *Chemical Engineering Science*, vol. 66, no. 6, pp. 1179–1188, 2011.

[24] J. Vicente, F. Topin, and J.-V. Daurelle, "Open celled material structural properties measurement: from morphology to transport properties," *Materials Transactions*, vol. 47, no. 9, pp. 2195–2202, 2006.